Thin Solid Films 624 (2017) 167–174

Contents lists available at ScienceDirect

Thin Solid Films

journal homepage: www.elsevier.com/locate/tsf

Effect of heat treating metallic constituents on the properties of $Cu_2ZnSnSe_4$ thin films formed by a two-stage process

M.A. Olgar [a,*], B.M. Başol [b], Y. Atasoy [a], M. Tomakin [c], G. Aygun [d], L. Ozyuzer [d], E. Bacaksız [a]

[a] Department of Physics, Karadeniz Technical University, 61080 Trabzon, Turkey
[b] Encore Solar, 6541 Via Del Oro, Suite B, San Jose, CA 95119, United States
[c] Department of Physics, Recep Tayyip Erdogan University, Rize, Turkey
[d] Department of Physics, Izmir Institute of Technology, Urla, Izmir, Turkey

ARTICLE INFO

Article history:
Received 9 July 2016
Received in revised form 20 January 2017
Accepted 20 January 2017
Available online 22 January 2017

Keywords:
$Cu_2ZnSnSe_4$ (CZTSe)
Sputtering
Soft-annealing
Kesterite
Thin film solar cells
Two-stage method

ABSTRACT

In this study $Cu_2ZnSnSe_4$ (CZTSe) thin films were grown by a two-stage process that involved sputter deposition of a Cu/Sn/Zn/Cu metallic stack, annealing the stack at various temperatures for 30 min, evaporation of a Se cap over the metallic stack thus forming a precursor layer, and subjecting the precursor layer to a final high temperature reaction step at 550 °C. Different samples were prepared with annealing temperatures of the metallic stacks ranging from 200 °C to 350 °C. The results showed that heat treatment of the metallic stacks did not cause much change in their morphology and elemental composition, however their phase content changed noticeably when the anneal temperature was raised to 250 °C. Specifically, while the metallic films were dominated by CuSn and Cu_5Zn_8 phases at low temperatures, the dominant phase shifted to Cu_6Sn_5 at the annealing temperature of 250 °C and higher. Also formation of a distinct Cu_3Zn_2 phase was observed upon annealing at temperatures at or above 250 °C. After reaction with Se, the CZTSe layer obtained from the metallic film, which was annealed at 250 °C was found to be the best n terms of its composition, crystalline quality and purity, although it contained a small amount of CuSe. The other layers were found to contain small amounts of other secondary phases such as SnSe, $CuSe_2$, ZnSe and Cu_2SnSe_3. SEM micrographs showed denser structure for CZTSe layers grown from metallic films annealed at or above 250 °C. Optical band gap, resistivity and carrier concentration of the best quality CZTSe film were found to be about 0.87 eV, 2 Ω-cm and 4×10^{17} cm^{-3}, respectively.

1. Introduction

Thin film solar cells based on Cu (In, Ga) Se_2 (CIGS) have shown significant improvement and attracted much attention due to their application in the photovoltaics industry. Although CIGS-based devices are to date the most efficient thin film solar cells with a champion conversion efficiency of 22.3% [1], limited supplies of In and Ga are expected to restrict manufacturing volume of this technology. One of the alternative compounds to replace CIGS in a solar cell structure is $Cu_2ZnSn(S,Se)_4$ (CZTS(e)) where In and Ga are substituted by tin (Sn) and zinc (Zn). CZTS(e) has drawn significant attention from the research community due to its composition comprising earth-abundant materials [2], its suitable direct band gap energy in the range of ~0.9 eV to 1.6 eV [3,4], and due to its high optical absorption coefficient ($\geq 10^4$ cm^{-1}). Although the theoretical efficiency of a CZTS(e)-based thin film solar cell is estimated to be over 30% [5], so far researchers could only demonstrate 10.4% conversion efficiency for $Cu_2ZnSnSe_4$ devices [6], and 12.6% for $Cu_2ZnSn(S,Se)_4$ based cells [7]. The reasons for this shortcoming are still being investigated.

Fabrication methods for CZTS(e) absorbers involve both vacuum and non-vacuum techniques. Vacuum methods include thermal evaporation [8], e-beam evaporation [9], pulsed laser deposition [10], and sputtering [11]. The non-vacuum methods include electrochemical deposition [12], spray pyrolysis [13], and sol-gel deposition [14]. Recently published work on CZTS(e) thin films include topics such as optimization of film growth parameters (e.g. annealing temperature/time [15]), investigation of composition effects on the film properties [16], and study of possible influence of using differently prepared stacked metallic precursor layers on the properties of the compound films grown by two-stage processes [17].

Gurav et al., in their 2013 study, showed that a soft-annealing treatment of Cu-Zn-Sn containing metallic layers produced by an electroplating method had significant influence on the properties of Cu_2ZnSnS_4 (CZTS) layers obtained from such layers after a high temperature sulfurization step [18]. In that study the metallic films were subjected to a soft-annealing process for 1 h at a temperature range of 250–350 °C and then sulfurized at 580 °C for 2 h. It was concluded

* Corresponding author.
E-mail address: maliolgar@ktu.edu.tr (M.A. Olgar).

http://dx.doi.org/10.1016/j.tsf.2017.01.037
0040-6090/

that the best soft-annealing temperature was 300 °C and such a treatment improved the properties of the resulting films. There has not been such a study yet investigating possible effects of soft-annealing on the properties of CZTSe layers grown by a two-stage technique. In this contribution we present data on the influence of relatively mild soft-annealing steps on the properties of CZTSe films obtained by reacting sputter deposited and annealed metallic stacks with Se.

2. Experimental

Kesterite CZTSe thin films were obtained by a two-stage process that involved high temperature annealing of precursor layers containing Cu, Zn, Sn and Se. Preparation of the precursor layers included the steps of: i) depositing Cu, Zn, and Sn onto unheated molybdenum (Mo) coated soda lime glass (SLG) substrates by DC magnetron sputtering from high-purity Cu (5 N), Sn (4 N), and Zn (4 N) targets in one pump-down to form metallic stacks, ii) heat treating the metallic stacks at various annealing temperatures, and iii) evaporating Se cap layers over the metallic films of step ii).

The base pressure of the sputtering chamber was about 10^{-6} mbar and the operating pressure was around 10^{-3} mbar. The metallic species were deposited on the substrates in the sequence of Cu/Sn/Zn/Cu to obtain the metallic stacks. Sputtering rate of each element was pre-determined through calibration runs and thickness measurements using a Veeco DEKTAK 150 surface profilometer. The total targeted thicknesses of the elemental films within the stack were 175, 165, and 230 nm for Cu, Zn, and Sn, respectively. Nearly 70% of the targeted Cu thickness was deposited over Mo, and the rest was placed over the Zn layer. The above-mentioned elemental metallic film thicknesses were targeted to yield compound layers with Cu-poor (Cu/Zn + Sn <1) and Zn-rich (Zn/Sn >1) compositions that are necessary for fabrication of efficient CZTSe type solar cells [7]. The metallic film thicknesses used were expected to yield about 1.4 μm thick compound layer based on the assumptions of 100% density and a compound density value of about 5.7 g/cm^3. The practical thickness values are expected to be larger than 1.4 μm.

Annealing of the metallic stacks was performed in a tube furnace in a static 5%H_2 + 95%Ar atmosphere at temperatures of 200, 250, 300, and 350 °C for 30 min. It should be noted that we selected milder annealing conditions compared to those employed by Gurav et al. [18] since their data indicated that a 60 minute anneal at temperatures at or above 300 °C caused appreciable Zn loss from the Cu-Zn-Sn films, which they compensated for by including excess Zn in their electroplated metallic layers. We did not include excess Zn in our stacks, but reduced the annealing time and also investigated the even lower annealing temperature of 200 °C in addition to higher temperatures.

The Se cap layers were deposited by thermal evaporation of Se (5 N) shots out of Mo boats. The base pressure of the evaporator was about 10^{-5} mbar and the operating pressure was around 10^{-4} mbar. Selenium thickness was monitored during the evaporation using an Inficon SQM 160 crystal controller/monitor. The targeted thickness of the Se layer was 1300 nm, which represented about 40% excess with respect to the amount that would be necessary to form the compound. This is because we determined, through calibration experiments, that excess Se was needed in the precursor layers to avoid formation of compounds with appreciable Se deficiency and associated secondary phases after the reaction step.

After the Se evaporation step, the (Cu-Zn-Sn)/Se precursor layers were reacted for 15 min in a tube furnace in a static 5%H_2 + 95%Ar atmosphere at 550 °C. For simulating a rapid thermal process, the tube furnace with the process gas was first heated to the reaction temperature and the samples were then rapidly pushed into the hot zone [11]. The estimated ramping rate of the temperature in these experiments was about 5 °C/s. In an effort to create an overpressure of Sn in the reaction environment we added Sn(II)Se powder with 4 N purity to the area around the samples on the sample holder.

In this manuscript the metallic stack samples are identified as CZT-AD, CZT-200, CZT-250, CZT-300 and CZT-350, and the compound layers obtained after the reaction step are marked as CZTSe-AD, CZTSe-200, CZTSe-250, CZTSe-300, and CZTSe-350. The 'AD' abbreviation refers to 'as-deposited' and the numerical values indicate the annealing temperatures for the metallic stacks. For example, CZT-350 implies a Cu/Sn/Zn/Cu metallic stack annealed at 350 °C for 30 min before the Se cap deposition and CZTSe-350 refers to the compound layer obtained by reacting the CZT-350/Se precursor structure at 550 °C for 15 min. It should be noted that the samples mentioned above were all produced from the same precursor structure (i.e. the sputtering and the Se evaporation steps were carried out during the same runs for all samples), only the metal stack annealing temperature being different. Since the CZTSe thin films were grown on conductive and non-transparent substrates, optical transmission and the electrical measurement in the plane of the films could only be performed after they were transferred from their substrates onto glass slides by transparent epoxy peeling approach as previously utilized by Basol [19]. The detailed experimental procedures used for mechanical transfer of the reacted films onto glass were described in our recent publication [11]. The crystalline structure and the structural quality of the films were determined by XRD measurements using a Rigaku SmartLab diffractometer with a CuKα radiation source (λ = 1.5405 Å) at room temperature. The phase compositions were also determined by Raman scattering measurements (Princeton Instruments, Acton SP2750 0.750 mm Imaging Triple Grating Monochrometer) excited with a laser at a wavelength of 488 nm. The morphological and compositional analyses were performed by a Jeol JSM 6610 scanning electron microscope (SEM) and an Oxford Instruments Inca X-act energy dispersive X-ray spectroscopy (EDX) system. The optical transmittance spectra were obtained using a Dongwoo Optron spectrophotometer in the wavelength range of 1000–1800 nm. The electrical characterization was performed using Van der Pauw method at room temperature. Electrical contacts in the Van der Pauw samples were made by Ag paste dots of about 1 mm diameter. The four electrical contacts were placed at the four corners of the 1 cm × 1 cm square samples.

3. Results and discussion

3.1. EDX

Various atomic ratios in the as-deposited and annealed metallic stacks, determined by EDX at an incident beam voltage of 25 kV are listed in Table 1. As can be seen from this table the as-deposited metallic stack is Cu-poor (Cu/Zn + Sn <1) and Zn-rich (Zn/Sn >1) as targeted, and this composition is retained in all of the annealed samples even for the highest anneal temperature of 350 °C. The Cu/(Zn + Sn) ratios for all the films are also relatively unchanged within the experimental error. These results are very different from the previously published work by Gurav et al., who found a drastic change (from 0.71 to 1.38) in the Cu/(Zn + Sn) ratio of their electroplated Cu-Zn-Sn films upon soft-annealing at 350 °C for 60 min [18]. As the results in Table 1 demonstrate, our sputter deposited films annealed by rapid thermal method for 30 min retained their composition well. Possible factors contributing

Table 1
Atomic ratios in metallic stacks as determined by EDX analysis.

Sample ID	Cu (%)	Zn (%)	Sn (%)	Cu/(Zn + Sn)	Zn/Sn
CZT-AD	45.4	29.7	24.9	0.83	1.19
CZT-200	44.2	30.2	25.6	0.79	1.17
CZT-250	43.9	30.4	25.7	0.78	1.18
CZT-300	43.6	29.4	27.0	0.77	1.08
CZT-350	43.7	29.4	26.9	0.77	1.09

to this result include, shorter annealing time and the different nature of our sputtered metallic stack films from the co-electroplated layers.

Table 2 gives the compositional information for the CZTSe layers obtained after the reaction step. As can be seen from this data, there is a trend of increasing Cu/(Zn + Sn) ratio upon reaction with Se. The Zn/Sn ratio, on the other hand shows a decrease by at most 0.19 for all samples, except for the CZTSe-250 sample, which appears to have retained its relatively Zn-rich composition. The small changes observed in the Zn/Sn ratios are indicative of some Zn loss from the compound layer during the selenization step. Although addition of Sn(II)Se in the reaction environment was to prevent Sn loss from the CZTSe structure, it may also have an impact on Zn-loss. Redinger et al. showed that Zn-loss can be observed with increasing of Se over pressure at high temperatures (>500 °C) [20]. It is not very clear why sample CZT-250 retained Zn more efficiently compared to the other samples during the reaction step. Differences between the annealed layers in terms of their phase content may have played a role in this as will be discussed later. Data in Table 2 also shows that all CZTSe layers have a Se/Metal ratio around 1. This is a necessary (but not sufficient) condition indicating that the selenization process has close to ideal conditions for obtaining CZTSe structure.

3.2. XRD

The XRD patterns obtained from the metallic stacks are presented in Fig. 1. Diffraction peak positions associated with elemental Sn (JCPDS 03-065-0296) and Cu (JCPDS 01-070-3038), and the binary metallic phases of Cu_6Sn_5 (JCPDS 03-065-2303), CuSn (JCPDS 03-065-3434), Cu_5Zn_8 (JCPDS 01-071-0397), Cu_3Zn_2 (JCPDS 25-0322), $CuZn_2$ (JCPDS 39-0400), and $CuZn_5$ (JCPDS 35-1152) are all marked on this figure along with the peak associated with Mo.

Yoo et al. had investigated secondary phase formation in CZTSe films by studying various film stacks by time-resolved XRD measurements as these stacks were heated up to a temperature of 550 °C [21]. The results showed that the tendency of reaction between the metallic pairs of elements could be expressed as Zn-Sn < Cu-Sn < Cu-Zn, meaning Cu-Zn reaction was the most favorable (taking place at the lowest temperature) followed by the reaction of Cu with Sn, and Zn with Sn. In another prior work, Wibowo et al. found that sputtered Cu/Sn/Zn stacks contained Cu_5Zn_8, Cu_6Sn_5, Sn, and Cu phases in their as-deposited form [22]. In our Cu/Sn/Zn/Cu stack we attempted to encourage the Cu-Sn and Cu-Zn reactions by splitting the Cu layer into two thinner sub-layers. Although it is difficult to say how much unreacted Cu is present in our films since the (111) reflection peak of Cu lies at around 43.29°, which is very close to the binary phases shown in Fig. 1, it is reasonable to assume that free Cu amount in our films would be smaller than those in reference [22] in light of the findings of Yoo et al. [21]. One can see a small peak at around 50.4° that gets even smaller as the metallic samples are heat treated at higher and higher temperatures. This peak is believed to belong to the (200) reflection of Cu. There is no evidence in Fig. 1 of a pure Zn phase, which is in agreement with the fact that Cu/Zn reaction is the most energetically favorable one and in our stack structure Cu is directly sputter deposited on Zn. The inset in Fig. 1 shows an expanded view of the major peak around 43° for the five different samples. It is interesting to note that the peak maxima is at higher angles for the CZT-AD and CZT-200 samples and it shifts to lower angles for samples annealed at or above 250 °C. It appears that the metallic films are dominated by CuSn and Cu_5Zn_8 phases at low temperatures, as signified by a broad peak at ~43.12°, and the dominant phase shifts to Cu_6Sn_5 with a sharper peak around ~42.98° at the annealing temperature of 250 °C and higher. The broad peak at low temperature samples, without doubt, has contribution from the unreacted Cu phase also. These results in general support the findings of Wibowo et al. who observed the XRD peak around 43° shifting to lower angles as the samples were heated up from room temperature to a temperature of 470 °C [22]. Another observation from Fig. 1 is the formation of a distinct Cu_3Zn_2 phase upon annealing at temperatures at or above 250 °C. For the lower temperature samples this phase appears as a shoulder of the main peak signifying a series of compositions present. It is also noted that the small Cu_5Zn_8 peaks at around 35° and 37.9° present in the low temperature films convert into minor $CuZn_2$ and $CuZn_5$ phases. In summary, the data in Fig. 1 demonstrates a noticeable change in the phase content of metallic films when the anneal temperature is increased to 250 °C.

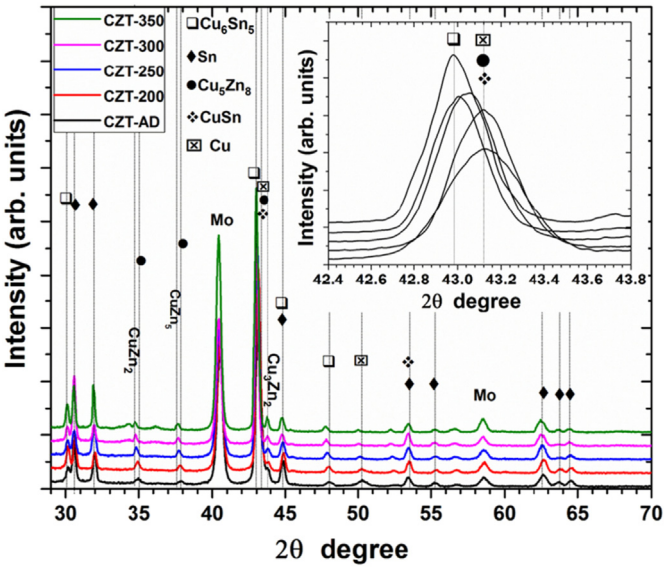

Fig. 1. XRD patterns of metallic stacks.

Table 2
Atomic ratios in CZTSe thin films as determined by EDX analysis.

Sample ID	Cu (%)	Zn (%)	Sn (%)	Se (%)	Cu/(Zn + Sn)	Zn/Sn	Se/metal
CZTSe-AD	22.9	13.5	13.1	50.4	0.86	1.03	1.02
CZTSe-200	22.6	13.5	13.8	50.1	0.83	0.98	1.00
CZTSe-250	22.2	14.9	12.4	50.5	0.82	1.20	1.02
CZTSe-300	23.2	12.9	13.1	50.7	0.89	0.98	1.03
CZTSe-350	22.8	13.0	13.2	50.2	0.87	0.99	1.02

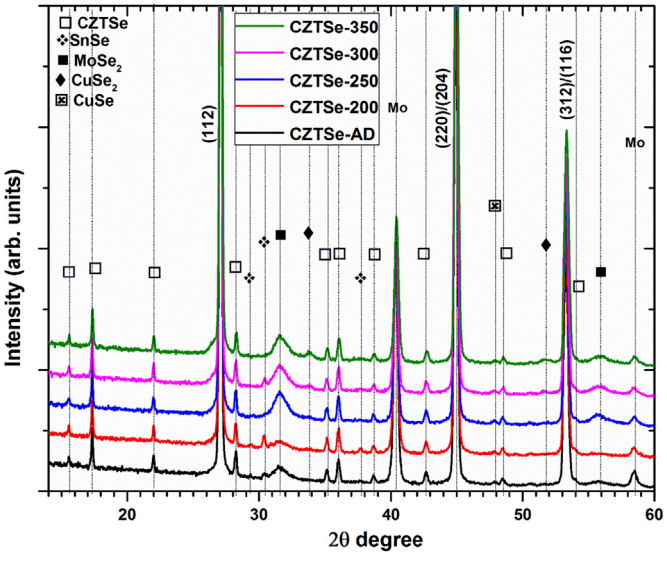

Fig. 2. XRD diffraction pattern of kesterite CZTSe thin films.

The XRD patterns of the CZTSe thin films, which were obtained after the CZT samples of Table 1 were reacted with Se, are displayed in Fig. 2. As can be observed from this data irrespective of the annealing temperature of the CZT samples, all five films show diffraction peaks at the expected positions of CZTSe 112 ($2\Theta = 27.15°$), 220/204 ($2\Theta = 45.10°$), and 312/116 ($2\Theta = 53.45°$) planes (JCPDS 01-070-8930). The estimated positions for the other lower intensity peaks of CZTSe with kesterite structure are also shown in the figure and they correlate well with the data. The Mo (JCPDS 01-089-5023) peak at 40.50° and the $MoSe_2$ (JCPDS 09-0312) peaks at around 31.55° and 55.87° are due to the substrate. Presence of $MoSe_2$ indicates reaction of the Mo layer with Se at 550 °C under the Se-rich conditions we provided during the reaction period. Moreover, additional peaks were observed for CZTSe-AD, CZTSe-200, CZTSe-300, and CZTSe-350 thin films, which may be attributed to SnSe (JCPDS 01-089-0236) and $CuSe_2$ (JCPDS 00-018-0453) phases. A considerably minor peak was observed around at 48° in all patterns, which may be attributed to CuSe (JCPDS 01-072-8417) [23]. Apart from the $MoSe_2$ and CuSe, which is highly conductive phase and has a detrimental effect on the cell performance, the CZTSe-250 sample yielded dominant characteristic diffraction peaks of CZTSe. Lack of secondary phases in this film correlates well with its desirable composition shown in Table 2.

Fig. 3 shows the full width at half maximum (FWHM) values obtained from the (112) peaks of Fig. 2. As can be seen from this figure the FWHM value goes down as the anneal temperature of the metallic films increases, reaching a minimum for the CZTSe-250 sample and then increases sharply for films annealed at higher temperatures. Decreasing FWHM can be correlated with improved crystallite size and lack of secondary phases that may contribute to the peak width. In that respect the CZTSe-250 sample appears to be the best quality film. The increase observed in the FWHM value for the CZTSe-350 sample may not signify a deterioration of the crystallite size in the material but rather it may be due to secondary phases (such as ZnSe, which has a 111 peak at $2\Theta = 27.22°$) that may broaden the 112 diffraction peak.

Although all of the reacted films of Fig. 2 showed characteristic peaks of CZTSe, their purity cannot be fully determined from this data since ZnSe (JCPDS 01-071-5977) and Cu_2SnSe_3 (CTSe) (JCPDS 01-072-8034) phases share a similar diffraction pattern with kesterite CZTSe. Additional complementary measurements utilizing Raman spectroscopy is required to further study the phase content of these CZTSe layers.

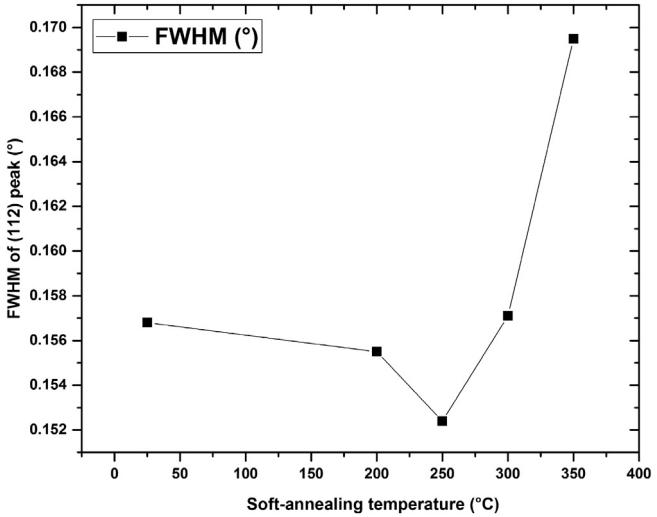

Fig. 3. FWHM values derived from the (112) peaks of CZTSe thin films of Fig. 2.

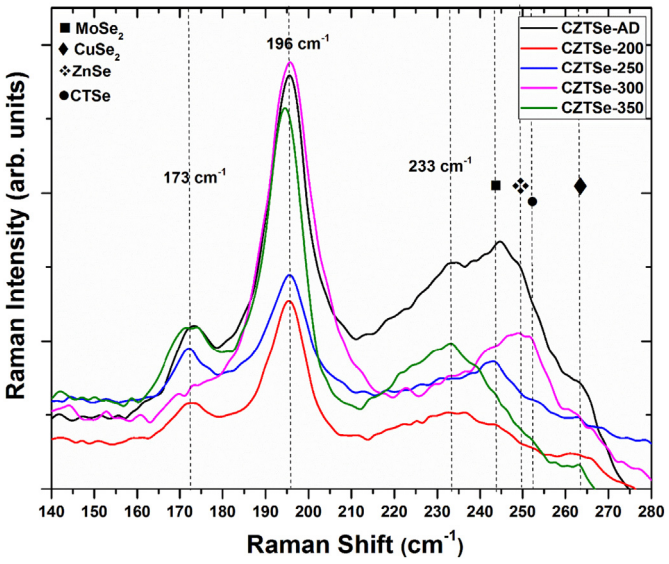

Fig. 4. Raman spectra of CZTSe thin films.

3.3. Raman spectroscopy

Fig. 4 presents the Raman spectra data collected from our CZTSe samples. Once again, it can be seen from the data of Fig. 4 that irrespective of the annealing temperature of the metallic stacks, the spectra of the reacted layers are dominated by two peaks located around at 196 cm^{-1} and 173 cm^{-1}. Both of these intense peaks are attributed to kesterite CZTSe phase.

The lower intensity characteristic peak at around 232–233 cm^{-1} also belongs to CZTSe [6]. A minor peak detected at 242–245 cm^{-1}can be attributed to $MoSe_2$ phase, which was also observed in the XRD pattern of Fig. 2. Unlike the other films, CZTSe-300 sample displayed a minor peak around at 250 cm^{-1} and 252 cm^{-1} which may be due to trace amounts of ZnSe and Cu_2SnSe_3 phases, which could not be distinguished by XRD [24–26]. The spectra of CZTSe-350 sample also show the presence of the $CuSe_2$ phase in support of the XRD data. This peak is not clearly seen for CZTSe-300 sample (which has the Cu-selenide phase according to the XRD data) due to the interference from other secondary phase peaks.

3.4. SEM

The SEM images taken from the surface and cross-section of the metallic precursor layers are given in Fig. 5. As can be seen from these SEMs although the metallic films were subjected to an annealing treatment step at various temperatures, the treatments did not change the morphology of the films much except that some fusion between the globules can be seen in the cross-section of sample CZT-350. This is because our annealing temperatures were below the melting temperature of Zn and the low melting Sn was sandwiched between two solid films of Cu/Cu-Sn alloys and Cu-Zn alloys during deposition.

Fig. 6 shows the top and cross-sectional view SEM images of the CZTSe layers. Irrespective of the annealing process before the reaction step, all of the films display non-uniform polycrystalline surface structures. The thickness values appear to be in the 1.4–2 μm range considering the fact that the cross sectional views are at 45° angle. CZTSe-AD thin film contains many voids that are visible in the surface SEM. Increasing the annealing temperature to 250 °C reduces the density of these voids giving rise to a more dense structure. Raising the annealing temperature above 250 °C causes appreciable change in the morphology of the reacted films. CZTSe-300 and CZTSe-350 samples display a rougher morphology with larger particle size and better fusion between the

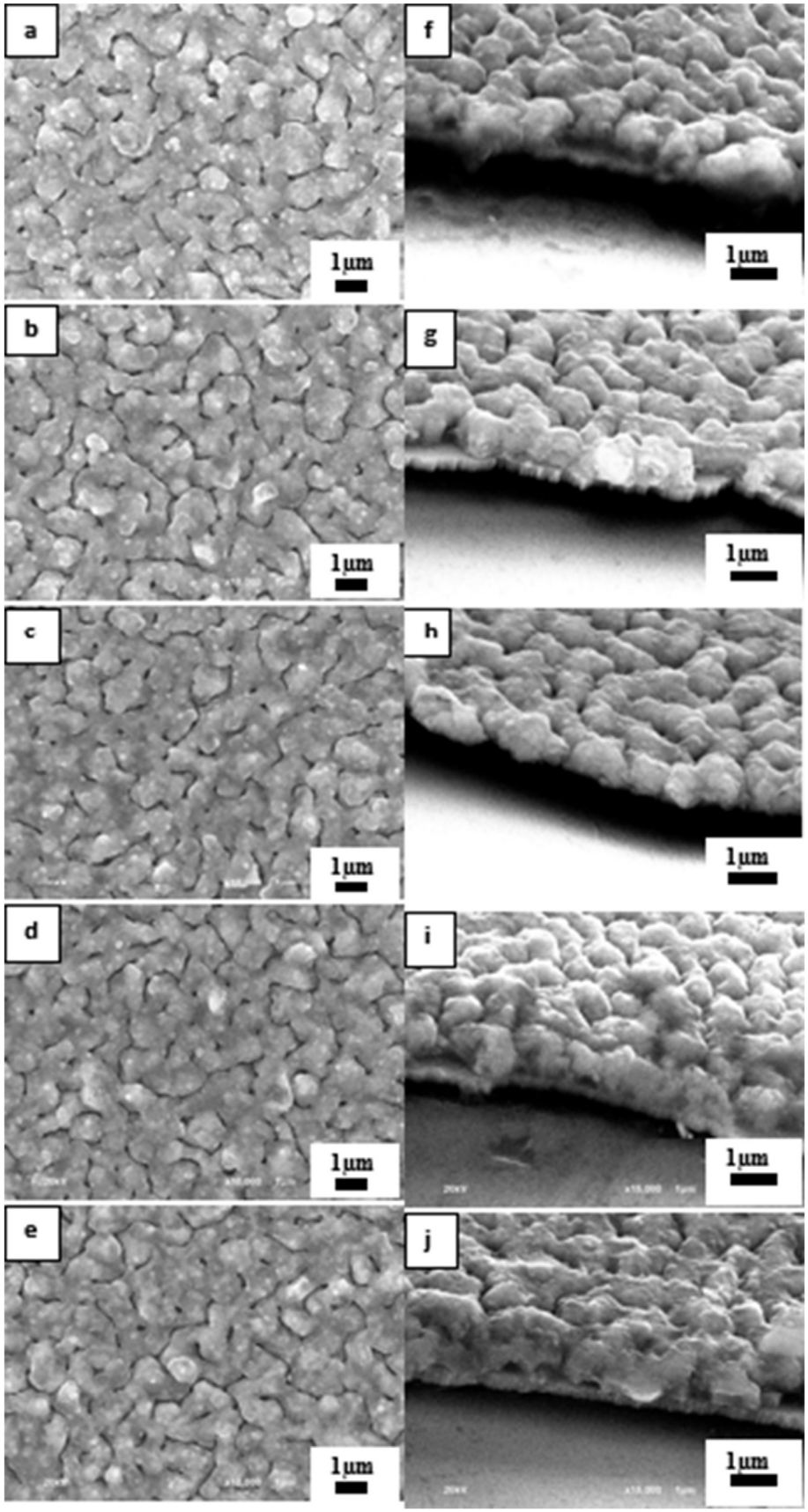

Fig. 5. Top and cross-sectional view SEMs of the metallic films; CZT-AD (a, f), CZT-200 (b, g), CZT-250 (c, h), CZT-300 (d, i), and CZT-350 (e, j).

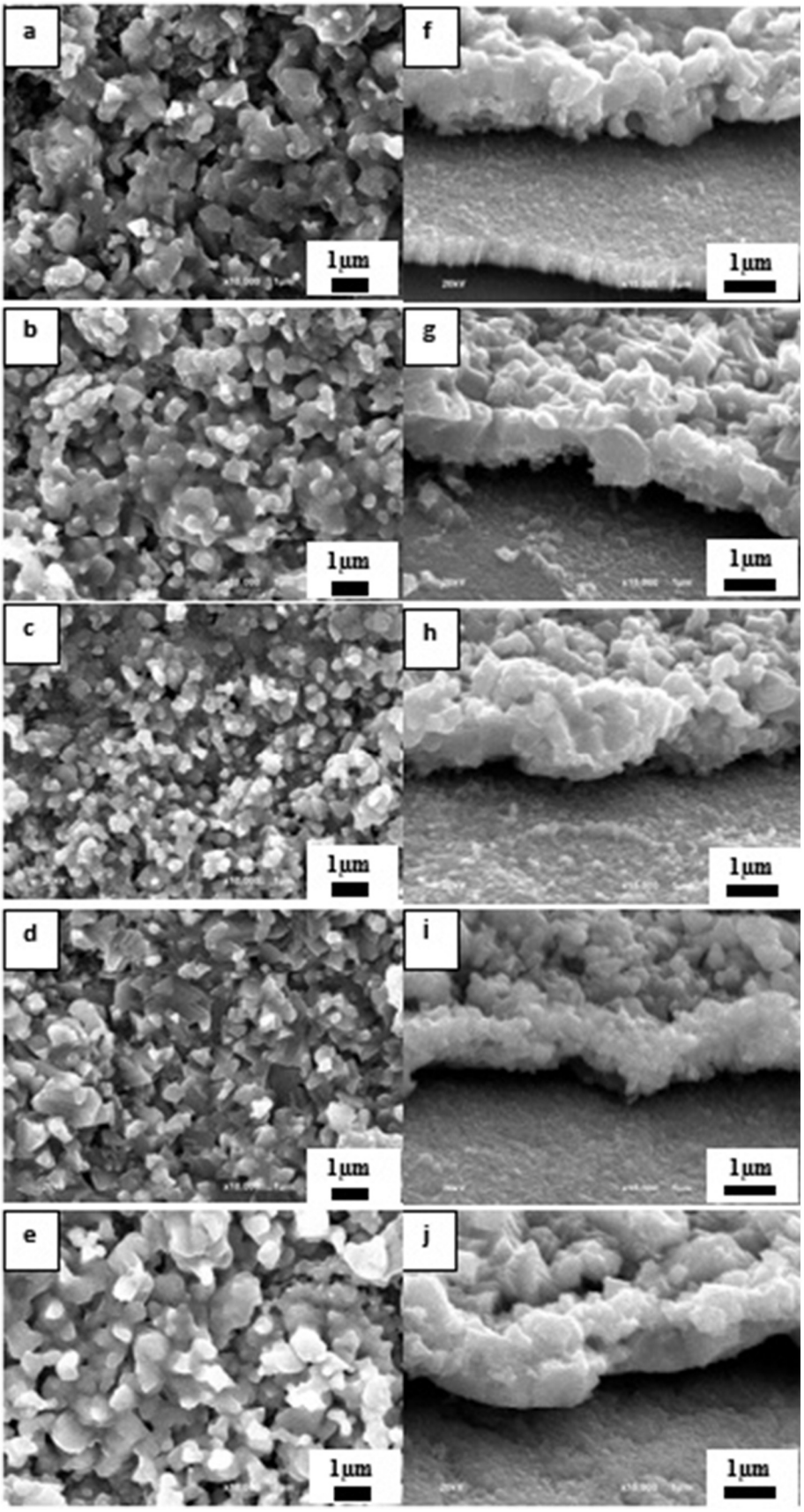

Fig. 6. Top and cross-sectional view SEMs of the reacted films; CZTSe-AD (a, f), CZTSe-200 (b, g), CZTSe-250 (c, h), CZTSe-300 (d, i), and CZTSe-350 (e, j) kesterite films.

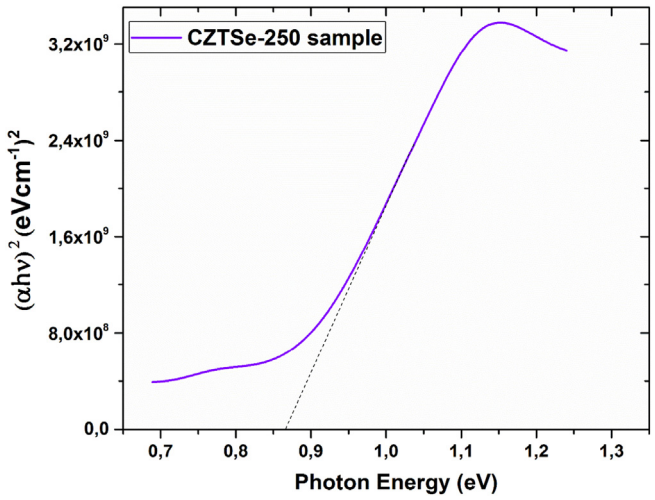

Fig. 7. Graph of $(\alpha h\upsilon)^2$ versus photon energy $(h\upsilon)$ for the CZTSe-250 sample.

surface features. This is expected since these films contain Cu-Se phase(s), which can act as low-melting fusing agents during the high temperature formation of the compound layer.

3.5. Optical and electrical properties

The optical band gap values for CZTSe films reported in the literature vary broadly (0.8–1.6 eV) and this variation has been attributed to the presence of appreciable amount of secondary phases (such as ZnSe and Cu_2SnSe_3) in some of the layers used in the bandgap measurements [27]. The optical band gap of the CZTSe-250 layer, which was our best quality film based on the characterization presented above, was determined from the $(\alpha h\upsilon)^2$ vs $(h\upsilon)$ curves (from the transmission measurements) using Eq. (1) [4];

$$\alpha h\upsilon = A\left(h\upsilon - E_g\right)^{1/2} \quad (1)$$

where α is the optical absorption coefficient, A is a constant, and E_g is the optical band gap. As shown in Fig. 7, the optical band gap value obtained by extrapolating the $(\alpha h\upsilon)^2$ vs $(h\nu)$ plot to the horizontal photon energy axis is about 0.87 eV.

The resistivity of the CZTSe-250 layer was measured using a square shaped Van der Pauw pattern with contacts at the four corners. The film had p-type conductivity and its resistivity and carrier concentration values were measured to be around 2 Ω-cm and 4×10^{17} cm^{-3}, respectively.

4. Conclusions

$Cu_2ZnSnSe_4$ (CZTSe) thin films grown by a two-stage process were characterized in terms of their structural, optical and electrical properties. The film growth approach included the steps of sputter depositing a Cu/Sn/Zn/Cu metallic stack, annealing the stack at temperatures of 200–350 °C for 30 min, evaporation of a Se cap over the metallic stack thus forming a precursor layer, and subjecting the precursor layer to a reaction step at 550 °C for 15 min. Influence of the metallic stack annealing process on the properties of the CZTSe layers obtained after the reaction step was studied through XRD, EDX, SEM and Raman spectroscopy measurements. The results showed that heat treatment of the metallic stacks did not cause much change in their morphology and the Cu-poor Zn-rich compositions, however their phase content changed noticeably when the anneal temperature was raised to 250 °C. After reaction with Se, the Zn content of the CZTSe layers were found to be lower except for the one obtained from the metallic film that was annealed at 250 °C. This CZTSe layer was also found to be the best in terms of its crystalline quality and purity, containing substantially just the kesterite CZTSe phase, other than a very small amount of CuSe. Other CZTSe layers were found to contain trace amounts of secondary phases such as SnSe, $CuSe_2$, ZnSe and Cu_2SnSe_3. SEM micrographs showed denser structure for CZTSe layers grown employing metallic films annealed at or above 250 °C. Optical band gap, resistivity and carrier concentration of the best quality film were found to be about 0.87 eV, 2 Ω-cm and 4×10^{17} cm^{-3}, respectively.

References

[1] J. Gifford, Solar Frontier hits 22.3% on CIGS cell, Industry and Suppliers, Market and Trends, 2015http://www.pv-magazine.com/news/details/beitrag/solar-frontier-hits-223-on-cigs-cell_100022342/#ixzz3v7SSqdiZ.
[2] S. Siebentritt, S. Schorr, Kesterites - a challenging material for solar cells, Prog. Photovolt. 20 (2012) 512–519.
[3] M. Altosaar, J. Raudoja, K. Timmo, M. Danilson, M. Grossberg, J. Krustok, E. Mellikov, $Cu_2Zn_{1-x}Cd_xSn(Se_{1-y}S_y)_4$ solid solutions as absorber materials for solar cells, Phys. Status Solidi (a) 205 (2008) 167–170.
[4] S. Yazici, M.A. Olgar, F.G. Akca, A. Cantas, M. Kurt, G. Aygun, E. Tarhan, E. Yanmaz, L. Ozyuzer, Growth of Cu_2ZnSnS_4 absorber layer on flexible metallic substrates for thin film solar cell applications, Thin Solid Films 589 (2015) 563–573.
[5] W. Shockley, H.J. Queisser, Detailed balance limit of efficiency of P-N junction solar cells, J. Appl. Phys. 32 (1961) 510–519.
[6] S. Oueslati, G. Brammertz, M. Buffiere, H. ElAnzeery, O. Touayar, C. Koble, J. Bekaert, M. Meuris, J. Poortmans, Physical and electrical characterization of high-performance $Cu_2ZnSnSe_4$ based thin film solar cells, Thin Solid Films 582 (2015) 224–228.
[7] W. Wang, M.T. Winkler, O. Gunawan, T. Gokmen, T.K. Todorov, Y. Zhu, D.B. Mitzi, Device characteristics of CZTSSe thin-film solar cells with 12.6% efficiency, Adv. Energy Mater. 4 (2014) 1301465.
[8] C.W. Shi, G.Y. Shi, Z. Chen, P.F. Yang, M. Yao, Deposition of Cu_2ZnSnS_4 thin films by vacuum thermal evaporation from single quaternary compound source, Mater. Lett. 73 (2012) 89–91.
[9] H. Araki, A. Mikaduki, Y. Kubo, T. Sato, K. Jimbo, W.S. Maw, H. Katagiri, M. Yamazaki, K. Oishi, A. Takeuchi, Preparation of Cu_2ZnSnS_4 thin films by sulfurization of stacked metallic layers, Thin Solid Films 517 (2008) 1457–1460.
[10] R.A. Wibowo, E.S. Lee, B. Munir, K.H. Kim, Pulsed laser deposition of quaternary $Cu_2ZnSnSe_4$ thin films, Phys. Status Solidi A 204 (2007) 3373–3379.
[11] M.A. Olgar, Y. Atasoy, B. Başol, M. Tomakin, G. Aygun, L. Ozyuzer, E. Bacaksız, Influence of copper composition and reaction temperature on the properties of CZTSe thin films, J. Alloys Compd. 682 (2016) 610–617.
[12] X. Zhang, X. Shi, W. Ye, C. Ma, C. Wang, Electrochemical deposition of quaternary Cu_2ZnSnS_4 thin films as potential solar cell material, Appl. Phys. A Mater. Sci. Process. 94 (2009) 381–386.
[13] Y.K. Kumar, G.S. Babu, P.U. Bhaskar, V.S. Raja, Preparation and characterization of spray-deposited Cu_2ZnSnS_4 thin films, Sol. Energy Mater. Sol. Cells 93 (2009) 1230–1237.
[14] K. Tanaka, Y. Fukui, N. Moritake, H. Uchiki, Chemical composition dependence of morphological and optical properties of Cu_2ZnSnS_4 thin films deposited by sol-gel sulfurization and Cu_2ZnSnS_4 thin film solar cell efficiency, Sol. Energy Mater. Sol. Cells 95 (2011) 838–842.
[15] H. Guan, H.L. Shen, C. Gao, X.C. He, Sulfurization time effects on the growth of Cu_2ZnSnS_4 thin films by solution method, J. Mater. Sci. - Mater. Electron. 24 (2013) 2667–2671.
[16] A.V. Moholkar, S.S. Shinde, G.L. Agawane, S.H. Jo, K.Y. Rajpure, P.S. Patil, C.H. Bhosale, J.H. Kim, Studies of compositional dependent CZTS thin film solar cells by pulsed laser deposition technique: an attempt to improve the efficiency, J. Alloys Compd. 544 (2012) 145–151.
[17] S.W. Shin, S.M. Pawar, C.Y. Park, J.H. Yun, J.H. Moon, J.H. Kim, J.Y. Lee, Studies on Cu_2ZnSnS_4 (CZTS) absorber layer using different stacking orders in precursor thin films, Sol. Energy Mater. Sol. Cells 95 (2011) 3202–3206.
[18] S.V. Gurav, S.M. Pawar, S.W. Shin, M.P. Suryawanshi, G.L. Agawane, P.S. Patil, J.H. Moon, J.H. Yun, J.H. Kim, Electrosynthesis of CZTS films by sulfurization of CZT precursor: effect of soft annealing treatment, Appl. Surf. Sci. 283 (2013) 74–80.
[19] B. Basol, Electrochemically deposited CdTe films and their application to solar cells, UCLA PhD Dissertation 1980, p. 34.
[20] A. Redinger, S. Siebentritt, Coevaporation of $Cu_2ZnSnSe_4$ thin films, Appl. Phys. Lett. 97 (2010) 092111.
[21] H. Yoo, R.A. Wibowo, G. Manoharan, R. Lechner, S. Jost, A. Verger, J. Palm, R. Hock, The formation mechanism of secondary phases in $Cu_2ZnSnSe_4$ absorber layer, Thin Solid Films 582 (2015) 245–248.
[22] R.A. Wibowo, S.A. Moeckel, H. Yoo, C. Hetzner, A. Hoelzing, P. Wellmann, R. Hock, Intermetallic compounds dynamic formation during annealing of stacked elemental layers and its influences on the crystallization of $Cu_2ZnSnSe_4$ films, Mater. Chem. Phys. 142 (2013) 311–317.
[23] M. Ganchev, J. Iljina, L. Kaupmees, T. Raadik, O. Volobujeva, A. Mere, M. Altosaar, J. Raudoja, E. Mellikov, Phase composition of selenized $Cu_2ZnSnSe_4$ thin films

determined by X-ray diffraction and Raman spectroscopy, Thin Solid Films 519 (2011) 7394–7398.
[24] P.M. Salomé, P.A. Fernandes, J.P. Leitão, M.G. Sousa, J.P. Teixeira, A.F. da Cunha, Secondary crystalline phases identification in $Cu_2ZnSnSe_4$ thin films: contributions from Raman scattering and photoluminescence, J. Mater. Sci. 49 (2014) 7425–7436.
[25] A.-J. Cheng, M. Manno, A. Khare, C. Leighton, S. Campbell, E. Aydil, Imaging and phase identification of Cu_2ZnSnS_4 thin films using confocal Raman spectroscopy, J. Vac. Sci. Technol. A 29 (2011) 051203.
[26] A. Redinger, K. Hönes, X. Fontané, V. Izquierdo-Roca, E. Saucedo, N. Valle, A. Pérez-Rodríguez, S. Siebentritt, Detection of a ZnSe secondary phase in coevaporated $Cu_2ZnSnSe_4$ thin films, Appl. Phys. Lett. 98 (2011) 101907.
[27] S. Ahn, S. Jung, J. Gwak, A. Cho, K. Shin, K. Yoon, D. Park, H. Cheong, J.H. Yun, Determination of band gap energy (Eg) of $Cu_2ZnSnSe_4$ thin films: on the discrepancies of reported band gap values, Appl. Phys. Lett. 97 (2010) 021905.